Measurement of the Viscosity of Guar Gum Solutions to 50,000 s^{-1} Using a Parallel Plate Rheometer

JEFFREY KRAMER, JONATHAN T. UHL, *and* ROBERT K. PRUD'HOMME

Department of Chemical Engineering
Princeton University
Princeton, New Jersey 08544

It is frequently necessary to measure the viscosity of polymer solutions at high shear rates to obtain data under the conditions encountered in industrial processes. Such measurements are most often made on a capillary viscometer. This paper presents a method of determining solution viscosities at shear rates up to 50,000 s^{-1} in a rotational rheometer using a parallel plate geometry. The two keys to performing these measurements are very small gaps between the parallel plates (on the order of 50 microns) to eliminate inertial secondary flows, and the ability to increase and decrease the shear rate quickly to minimize viscous heating. A technique for setting and measuring small gaps is presented. Possible sources of error including inertia, axial compliance, and viscous heating are analyzed. A comparison is made between the viscosity of a 0.7 percent hydroxypropyl guar (HPG) solution measured on the parallel plate rheometer and the viscosity measured in a capillary viscometer. Viscosities of HPG solutions having concentrations of 0.25, 0.50, 1.00, and 1.45 percent are presented over the shear rate range 100 to 50,000 s^{-1}.

INTRODUCTION

Guar gum is an edible water-soluble carbohydrate composed primarily of mannose and galactose sugars (1). The ability of guar gum to act as an efficient water thickening agent at low concentrations, its relatively low cost, and its edibility make it commercially attractive. The food industry makes widespread use of guar gum as a thickener for ice cream, sauces, and salad dressings. In the oil and gas industry, guar is used in fracturing fluids where its high viscosity enables it to carry graded sand into rock fractures. Flow of HPG fracturing fluids through perforations in the well casings involves shear rates in the range of 50,000 s^{-1}.

In the early sixties, Merrill and coworkers ran a series of shear experiments on polystyrene and polyisobutylene solutions utilizing a concentric cylinder geometry and small gap separations (approx. 125 microns) to reach high shear rates (2–6). However, the primary means of high shear rate analysis has remained the capillary viscometer.

This paper presents a method using a rotational parallel plate geometry to determine high shear rate solution viscosities. Connelly and Greener (7) have independently investigated similar parallel plate measurements. We have adopted their suggestion for the use of a shear rate ramp test mode (to be discussed below), and here we present a graphical method for determining small gap separations from measurements of torque and rotational speed at several gap spacings. Experiments were conducted on a Rheometrics System IV rheometer (Rheometrics Inc., Piscataway, N.J.). The configuration consists of two parallel flat disks separated by a gap distance δ. The top disk is rotated at an angular speed ω while the bottom disk remains stationary (*Fig. 1*). The torque and normal forces produced are measured by a transducer connected to the stationary plate.

The viscosity of the fluid can be determined from torque measurements using an analysis that is given in standard references (8).

$$\eta(\dot{\gamma}_R) = \frac{(T/2\pi R^3)}{\dot{\gamma}_R}\left[3 + \frac{d\ \ln(T/2\pi R^3)}{d\ \ln\ \dot{\gamma}_R}\right] \quad (1)$$

where:

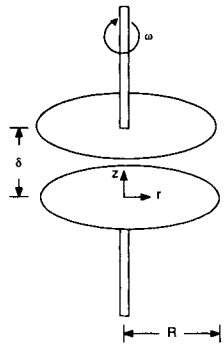

Fig. 1. Diagram of parallel plate geometry.

T = Torque on the stationary disk
$\dot{\gamma}_R$ = shear rate at the edge of the disk ($=R\omega/\delta$)
δ = gap separation
ω = angular velocity
R = radius of the disk.

The viscosity of the test solution can then be determined from a knowledge of the torque and the shear rate at the edge of the plate.

TECHNIQUES FOR NARROW GAP MEASUREMENTS

To achieve the high shear rates desired (50,000 s^{-1}), it is necessary to use as small a gap as possible for three reasons. First, for a fixed rotational speed, the smaller the gap the larger the shear rate obtained. Secondly, a small gap setting minimizes secondary flow which will be discussed later. And thirdly, small gaps facilitate heat conduction to the walls and thereby minimize errors arising from viscous heating. Experience shows that a gap distance of 50 microns could be used.

The usual method of determining the gap distance (δ) on the System IV rheometer is to close the disks until they are in contact, zero a digital gap indicator which is accurate to within one micron, and then separate the plates until the desired spacing is achieved. For large gaps (i.e. greater than 200 microns) this method is satisfactory. However, for small gap measurements either imperfect alignment of the disks or imperfections on the disk surfaces cause the disks to come into contact with each other in a small area while the major portion of the disks are still separated. In other words, the zero setting on the gap indicator would be in error by an amount which we designate as ϵ_0. *Figure 2* shows the shear stress *vs.* commanded gap separation for glycerin at a commanded shear rate of 1000 s^{-1} using the 50 mm diameter parallel plate geometry.

We have developed the following calibration technique to determine the effective gap spacing. The method is similar to that proposed by Connelly and Greener (7) where we use a graphical method that permits a check on the quality of the data and the errors in gap spacing. For a Newtonian fluid the viscosity can be determined from the measured torque by:

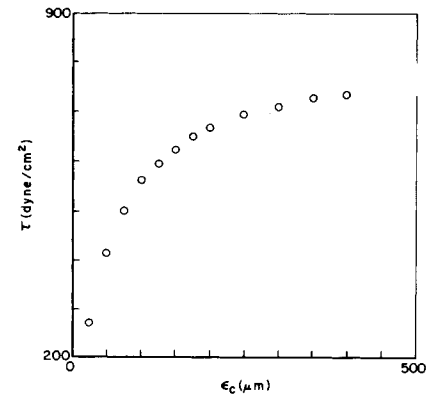

Fig. 2. Shear stress, τ, vs. parallel plate gap separation, ϵ_c, for glycerin at a commanded shear rate of 1000 s^{-1}.

$$T = \frac{\pi R^3}{2}\dot{\gamma}_R\eta \tag{2}$$

which defines a stress $\langle\tau\rangle$,

$$\langle\tau\rangle = \frac{2T}{\pi R^3} = \dot{\gamma}_R\eta \tag{3}$$

In the operation of the System IV rheometer, the operator enters a value for the commanded shear rate $\dot{\gamma}_c$ and a commanded gap separation δ_c. The System IV then measures the torque and calculates the viscosity from *Eq 2* by assuming $\dot{\gamma}_R = \dot{\gamma}_c$. However, the commanded shear rate based on the commanded gap setting is incorrect due to the error in the gap separation. The true gap separation is the specified gap δ plus the gap error ϵ_0. The value of this gap error can be calculated in the following manner. The actual shear rate $\dot{\gamma}_R$ is related to the experimentally measured stress $\langle\tau\rangle$ by,

$$\langle\tau\rangle = \eta\dot{\gamma}_R = \frac{\eta\omega R}{\delta_c + \epsilon_0} \tag{4}$$

Next we substitute for the angular velocity and radius in terms of the commanded shear rate and gap separation; that is, $\gamma_c = \omega R/\delta_c$, to obtain,

$$\langle\tau\rangle = \frac{\eta\dot{\gamma}_c\delta_c}{\delta_c + \epsilon_0} \tag{5}$$

Rearranging the above gives:

$$\frac{\dot{\gamma}_c\delta_c}{\langle\tau\rangle} = \left(\frac{1}{\eta}\right)\delta_c + \left(\frac{\epsilon_0}{\eta}\right) \tag{6}$$

Data are plotted as $\dot{\gamma}_c\delta_c/\langle\tau\rangle$ *vs.* δ_c, as suggested by *Eq 6* to give a slope of $(1/\eta)$ and an intercept of (ϵ_0/η). *Figure 3* shows the data from *Fig. 2* replotted in this manner.

Once the value of the gap error has been determined it is used as the new zero. For example, from *Fig. 3* the gap error was found to be 49 microns and a gap of 50 microns was desired. To get the desired separation, the gap indicator would be set to only 1 micron. With

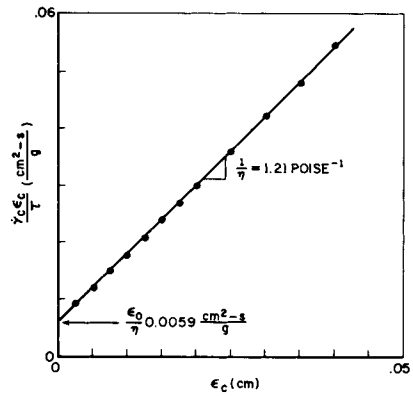

Fig. 3. Data from Fig. 1 replotted using Eq 6.

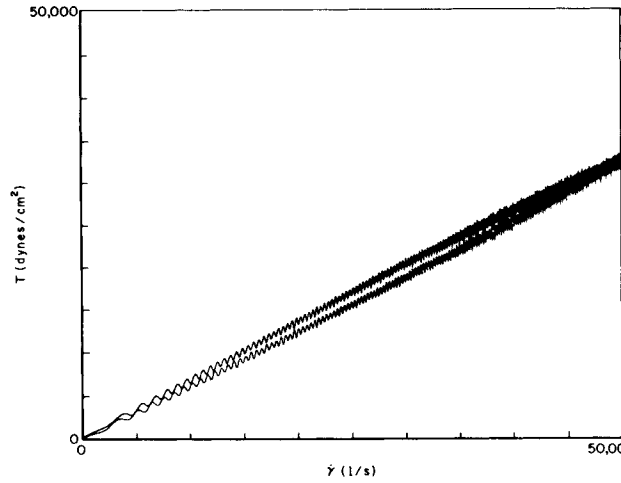

Fig. 4. Plot showing hysteresis due to the effect of viscous heating on a glycerin sample. Gap separation is 50 microns. Time to maximum shear is 20 s.

careful alignment of the system the measured gap errors are generally less than 40 microns.

At high shear rates, viscous heating can cause viscosity errors for fluids with temperature sensitive viscosities. To insure that viscous dissipation did not cause an error in the measured viscosity, a thixotropic loop method suggested by R. W. Connelly and J. Greener (7) was adopted. In a thixotropic loop test, which can be run on the System IV rheometer, the shear rate is increased over a period of time t_1 to a specified value and then immediately decreased over the same time period to the original shear rate. If viscous heating is negligible the plot of stress *vs.* shear rate for the increasing shear rate period should coincide with the plot for the decreasing shear rate period. If viscous heating is important the measured viscosity during the decreasing period will be less than that of the increasing period and hysteresis will be observed as shown in *Fig. 4*.

By examining thixotropic runs with total times for the loop of 4 s, 10 s etc, for evidence of a hysteresis, the time scale for which viscous heating effects can be neglected, t_v, can be experimentally determined. Thereafter, all the experiments are run at times shorter than t_v.

Though viscous energy dissipation occurs uniformly across the gap, energy is only removed at the top and bottom plate. This might lead to temperature gradients within the gap. The time constant for heat conduction in the parallel plate is given by:

$$\tau = \frac{\rho C_p \delta^2}{k} \tag{7}$$

which is equal to 0.016 s. The very small gap settings used cause the time for thermal conduction to the walls to be very short.

SOURCES OF EXPERIMENTAL ERROR

Secondary flow effects

For inelastic fluids in the absence of inertia, the flow between rotating parallel plates involves only tangential velocity components. At high rotation rates inertia forces the fluid radially outward near the moving plate which draws fluid radially inward near the stationary plate. This creates a secondary flow field superimposed on the tangential field. The magnitude of the secondary flow is governed by the Reynolds number, *Re*, defined:

$$Re = \frac{\rho \dot{\gamma}_R \delta^2}{\eta} \tag{8}$$

It can be seen that decreasing the gap separation greatly decreases the Reynolds number at a fixed shear rate.

Turian (9) has used a perturbation scheme to solve the equations of motion for secondary effects in a Newtonian fluid. His solution agrees well with published data. For a parallel plate system the measured torque T divided by the torque in absence of secondary flow, T_0, is given by:

$$\frac{T}{T_0} = 1 + \frac{3}{4900} Re^2 + \cdots \tag{9}$$

Where the $0(Re^2)$ term accounts for the effect of secondary flows. In our experiments for the 0.7 percent guar solution at 50,000 s^{-1} the increase in torque is expected to be $T/To = 1.15$. While the analysis was developed for Newtonian fluids and is not strictly applicable to shear thinning fluids, it is presented in order to provide an estimate of when secondary flow effects start to influence torque measurements.

Axial Compliance

As indicated in the secondary flow section, significant normal forces can develop at high shear rates. A positive normal force contribution arises from the elasticity of the fluid, whereas a negative contribution arises from the inertial forces. In our experiments the inertial forces dominate. The lower pressure seen at the center of the disks can cause the gap separation to decrease. Uhl (10) found the normal compli-

ance of the 19.6 *N* (2,000 g_f) melt transducer for the System IV rheometer to be 0.0101 microns/g_f. With a knowledge of the magnitude of the normal forces present, this value can be used to correct for gap separation errors. The System IV software does not provide normal force values for a thixotropic loop experiment. However, normal force values obtained from steady shear experiments at 50,000 s^{-1} provide an estimate of the compliance error for the thixotropic loop. Negative normal forces of 2.15 *N* (220 g_f) were measured at 50,000 s^{-1} in steady shear experiments for a gap separation of 50 microns; this value leads to a 4 percent error in the gap separation.

Capillary Viscometer

The results obtained using the rotational rheometer were compared with data obtained from a capillary viscometer. The fluid viscosity is calculated from measurements of flow rate, Q, and pressure drop, ΔP, using the "Weissenberg-Rabinowitch" equation (11):

$$\eta(\dot{\gamma}_R) = \frac{\tau_R}{\dot{\gamma}_R} = \frac{\tau_R}{(Q/\pi R^3)}\left[3 + \frac{d\ \ln(Q/\pi R^3)}{d\ \ln\tau_R}\right]^{-1} \quad (10)$$

where τ_R is the wall shear stress defined by,

$$\tau_R = \frac{R\Delta P}{2L} \quad (11)$$

The shear rate is calculated from:

$$\dot{\gamma} = \frac{1}{\tau_R^2}\frac{d}{d\tau_R}\left(\tau_R^3\frac{Q}{\pi R^3}\right) \quad (12)$$

The experimental apparatus used in the experiment consists of a high pressure cell connected to a capillary of a known radius and length (*Fig. 5*). The driving force is produced by pressurized nitrogen. The actual pressure drop is recorded by both a gage and pressure transducer (Celesco model P7D differential pressure transducer). Flow rate measurements are made by collecting a sample of solution over a known period of time and converting to volumetric units by using the measured density of the solution.

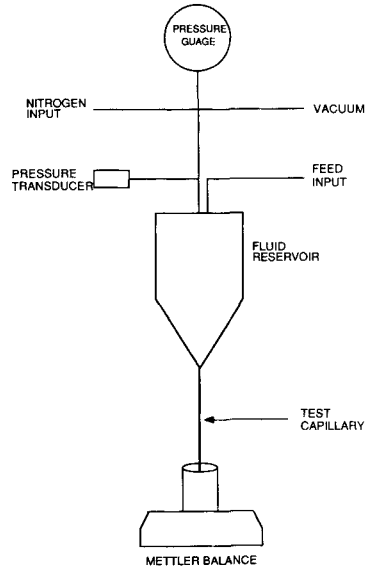

Fig. 5. Schematic diagram of capillary viscometer apparatus.

In *Eq 11* for stress at the wall, both the pressure drop and the capillary length are easily measured. However, in order to measure the small capillary radius accurately it is necessary to perform the following calibration experiment.

The equation for the flow rate of a Newtonian fluid in laminar flow can be rearranged to determine the radius of the tube:

$$R = \left(\frac{8Q\eta L}{\pi\Delta p}\right)^{1/4} \quad (13)$$

Using a Newtonian fluid of known viscosity, several experiments at varying pressure drops were run to determine an average tube radius. The radius determined from these experiments was 1.69×10^{-4} m with a standard deviation of ±10 percent. Viscosities calculated using the capillary viscometer values of the radius are shown in *Fig. 6* along with the viscosities measured on the System IV rheometer using the narrow gap technique.

RESULTS

Figure 7 shows the stress *vs.* shear rate data from a thixotropic loop test for the guar solution. The stress measured during the increasing and decreasing segments of the thixotropic loop experiment lie on top of one another. This indicates that viscous heating effects were unimportant for this shear rate and time range. The large oscillations in stress are due to the plate surfaces not being exactly parallel and/or the plate surfaces not being perfectly flat. The magnitude of the oscillations depends on the

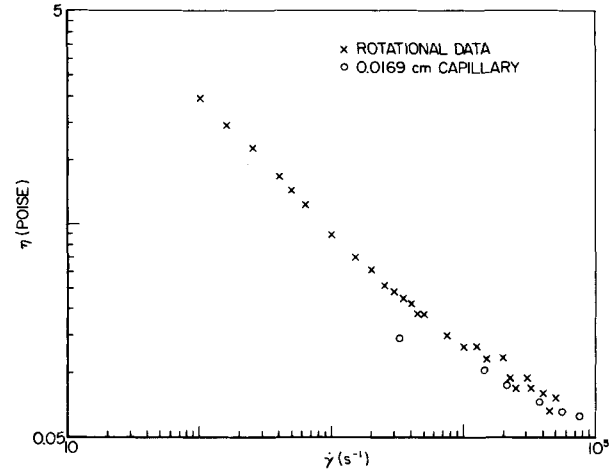

Fig. 6. Plot of System IV parallel plate viscosity data over shear rate range of 100 to 50,000 s^{-1}. For comparison, data calculated from a capillary viscometer is also shown.

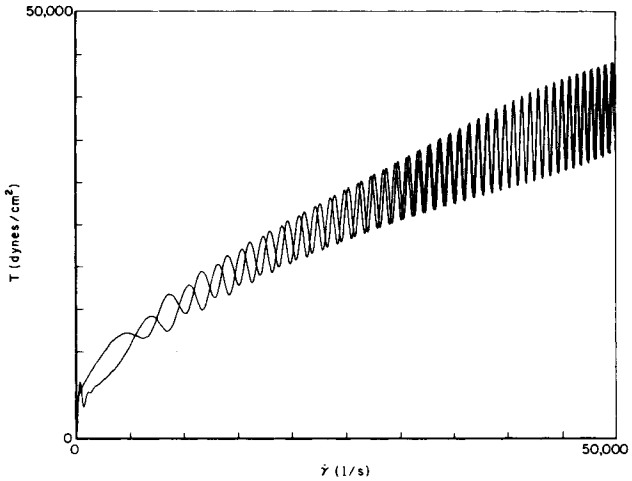

Fig. 7. Plot of a thixotropic loop experiment. Sample is a 0.7 percent guar solution. Time to maximum shear is 5 s. This plot shows no evidence of a hysteresis indicating that viscous heating effects are negligible.

ratio of the total gap setting to the gap error ϵ_0. If this ratio is close to one then at some point as the disks rotate they will pass very close to each other and the shear rate, and therefore the stress, will be very high. This would cause the torque to vary sinusoidally. A further support of this observation is that the frequency of the oscillation increases as the rotational speed increases. To get an average reading for the slope in *Eq 1*, a line is drawn down the center of the oscillations in a log-log plot. Over certain ranges of the shear rate a straight line is a good approximation (*Table 1*). From these slopes, viscosities are calculated and plotted in *Fig. 6.*

Upon examination of this data, one sees that it can be fairly well described by a power law region below 20,000 s^{-1}. Above 20,000 s^{-1} the viscosity decreases but less quickly. The viscosity at 100 s^{-1} is 2.1 poise but has dropped to 0.07 poise at 50,000 s^{-1}. Clearly it would be impossible for the viscosity to continue decreasing indefinitely as suggested by the power law model since at 60,000 s^{-1} the viscosity of the solution would equal that of water if the viscosity were calculated from the power-law parameter determined in the range 100 $s^{-1} < \dot{\gamma} <$ 20,000 s^{-1}.

For comparison, data from the capillary viscometer for the average radii is plotted. As described in the capillary apparatus section, the viscosity calculations are very sensitive to the radius dimension used. Due to the high sensitivity of the capillary viscosity data to the radius we have more confidence in the rotational data.

The effect of polymer concentration on the high shear rate viscosity is illustrated for solutions of 0.25, 0.50, 1.0, and 1.45 percent HPG in *Fig. 8.* The sample preparation and the experimental procedure for these runs were the same as those used for the 0.7 percent HPG solution. As can be seen from *Fig. 8*, the data

Table 1.

Shear Rate (1/s)	Slope
500–2,500	0.40
2,500–5,000	0.49
5,000–15,000	0.51
15,000–50,000	0.61

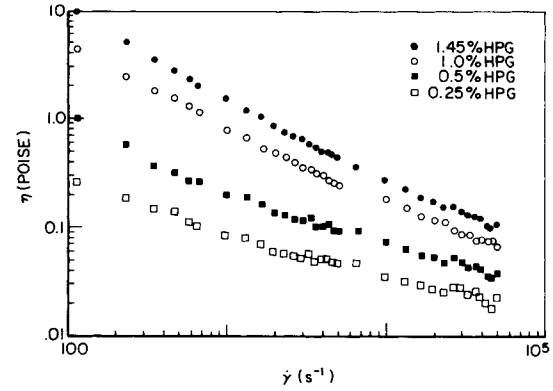

Fig. 8. Viscosity vs. shear rate data for HPG solution concentrations of 0.25, 0.50, 1.00, and 1.45 percent.

follows the same pattern as that of the 0.7 percent HPG. The data clearly shows that as the concentration of HPG is increased, the measured viscosity increases at all shear rates. For example, at 110 s^{-1} the viscosity increases in the series 0.25, 0.96, 4.2, and 9.5 poise as one varies the concentrations from 0.25 to 1.45 percent HPG.

CONCLUSION

The above discussion demonstrates an accurate method of viscosity determination at high shear rates on a parallel plate rotational rheometer. Errors due to viscous heating and secondary flows can be minimized using small gaps and a thixotropic loop shear history. Data for a 0.7 percent HPG solution has been presented and compared with capillary viscometer experiments. Additional data for 0.25, 0.50, 1.00, and 1.45 percent HPG solutions are included.

REFERENCES

1. "Handbook of Water Soluble Gums and Resins," Ch. 6, McGraw Hill, (1980).
2. E. W. Merrill, *J. Polym. Sci.*, **38**, 539 (1959).
3. E. W. Merrill, A. Ram, and H. S. Mickley, *J. Polym. Sci.*, **51**, 43 (1961).
3. E. W. Merrill, H. S. Mickley, A. Ram, and G. Perkinson, *Trans. Soc. Rheol.*, **5**, 237 (1961).
5. E. W. Merrill, H. S. Mickley, A. Ram, and W. M. Stockmayer, *Trans. Soc. Rheol.*, **6**, 119 (1962).
6. E. W. Merrill, H. S. Mickley, A. Ram, and W. M. Stockmayer, *J. Polym. Sci.*, **A-1**, 1201 (1963).
7. R. W. Connelly, and J. Greener, *J. Rheol.*, **29**, 209 (1985).
8. "Dynamics of Polymeric Liquids," pp. 176–179, John Wiley & Sons, New York (1977).
9. R. Turian, *Ind. Eng. Chem. Fundam.*, **11**, 3 (1972).
10. J. T. Uhl, Ph.D. Thesis, Princeton Univ. (1983).
11. "Dynamics of Polymeric Liquids," pp 179–182, John Wiley & Sons, New York (1977).